Deletion of the chloride transporter Slc26a9 causes loss of tubulovesicles in parietal cells and impairs acid secretion in the stomach

Jie Xu[a,b,1], Penghong Song[c,1,2], Marian L. Miller[d], Frank Borgese[e], Sharon Barone[b], Brigitte Riederer[c], Zhaohui Wang[b], Seth L. Alper[f], John G. Forte[g], Gary E. Shull[h], Jordi Ehrenfeld[e], Ursula Seidler[c], and Manoocher Soleimani[a,b,i,3]

[a]Research Services, Veterans Affairs Medical Center, Cincinnati, OH 45220; Departments of [b]Medicine, [d]Environmental Health, and [h]Molecular Genetics and Biochemistry, and [i]Center on Genetics of Transport and Epithelial Biology, University of Cincinnati, Cincinnati, OH 45267; [c]Department of Gastroenterology, Hepatology, and Endocrinology, University of Hannover, 30625 Hannover Germany; [e]Centre National de la Recherche Scientifique/Université de Nice Sophia Antipolis, 06108 Nice, France; [f]Renal Division, Harvard University Medical School, Boston, MA 02115; and [g]Department of Molecular and Cell Biology, University of California, Berkeley, CA 94720

Edited by Richard P. Lifton, Yale University School of Medicine, New Haven, CT, and approved September 24, 2008 (received for review January 23, 2008)

Slc26a9 is a recently identified anion transporter that is abundantly expressed in gastric epithelial cells. To study its role in stomach physiology, gene targeting was used to prepare mice lacking Slc26a9. Homozygous mutant (Slc26a9$^{-/-}$) mice appeared healthy and displayed normal growth. Slc26a9 deletion resulted in the loss of gastric acid secretion and a moderate reduction in the number of parietal cells in mutant mice at 5 weeks of age. Immunofluorescence labeling detected the H-K-ATPase exclusively on the apical pole of gastric parietal cells in Slc26a9$^{-/-}$ mice, in contrast to the predominant cytoplasmic localization in Slc26a9$^{+/+}$ mice. Light microscopy indicated that gastric glands were dilated, and electron micrographs displayed a distinct and striking absence of tubulovesicles in parietal cells and reductions in the numbers of parietal and zymogen cells in Slc26a9$^{-/-}$ stomach. Expression studies indicated that Slc26a9 can function as a chloride conductive pathway in oocytes as well as a Cl^-/HCO_3^- exchanger in cultured cells, and localization studies in parietal cells detected its presence in tubulovesicles. We propose that Slc26a9 plays an essential role in gastric acid secretion via effects on the viability of tubulovesicles/secretory canaliculi and by regulating chloride secretion in parietal cells.

acid secretion | chloride channel | acid-base transporter | chloride/bicarbonate exchanger

Gastric acid production originates in the parietal cell through the coordinated operation of apical and basolateral membrane transport proteins (1–9). The apical secretory machinery includes the gastric H-K-ATPase, a chloride channel, and a K^+ recycling pathway (1–9). Despite an essential role for the apical Cl^- channel in gastric acid secretion, its molecular identity remains unknown. Although ClC-2 was suggested as a likely candidate (10, 11), recent reports have questioned the apical localization and role of ClC-2 in gastric acid secretion (12, 13).

SLC26 (human)/Slc26 (mouse) homologs are members of a conserved family of anion exchangers that display selective and limited tissue expression in epithelial cells (14–22). Several SLC26 members can function as chloride/bicarbonate exchangers. These include SLC26A3 (DRA), SLC26A4 (pendrin), SLC26A6 (PAT1 or CFEX), SLC26A7, and SLC26A9 (23–27). SLC26A7 and SLC26A9 can also function as chloride (anion) conductive pathways (28–30).

SLC26A9/Slc26a9 is expressed predominantly in the stomach and lung (27). The expression of Slc26a9 in the stomach is limited to surface epithelial cells and cells deeper in gastric glands that appeared to be parietal cells (27), whereas its expression in the lung is detected in alveolar and tracheal epithelial cells (20). Slc26a9 expression was reduced significantly in the stomach of NHE2-null mice (27), which exhibit achlorhydria and a severe reduction in gastric parietal cells with aging (31), consistent with the expression of Slc26a9 in parietal cells. Here, we show that targeted ablation of Slc26a9 causes achlorhydria, indicating that it plays a critical role in gastric acid secretion.

Results

Generation of Slc26a9-Null Mutant Mice. The Neo cassette replaces 4.0 kb of the gene, including exons 2–5, which contain the ATG initiation codon in exon 2 (Fig. 1, *A* and *B* and *Experimental Procedures*). Targeted ES cells (Fig. 1*C*) were used to generate chimeric mice that were bred to obtain wild-type (Slc26a9$^{+/+}$), heterozygous (Slc26a9$^{+/-}$), and null (Slc26a9$^{-/-}$) mice (Fig. 1*D*). Slc26a9$^{-/-}$ mice exhibited normal growth and survival relative to wild-type littermates. In addition, both male and female Slc26a9$^{-/-}$ mice were fertile.

Analysis of Histopathologic and Ultrastructural Changes in Slc26a9-Null Gastric Mucosa. H&E staining revealed dilated gastric glands in 5- to 6-week-old Slc26a9$^{-/-}$ mice. The glands contained lucent contents, and some parietal cells seemed flattened (Fig. 2*A Center* and *Right* vs. *Left*). Parietal cells (Fig. 2*A*, blue arrow) with their lighter cytoplasm and distinct organization were present at ≈40% of the numbers found in Slc26a9$^{+/+}$ mice (WT, 41.2 ± 3.2, $n = 3$ vs. KO, 16.25 ± 1.15, $n = 3$; $P < 0.01$) (Fig. 2*A Center* and *Right* vs. *Left*). Zymogen cells (Fig. 2*A*, white arrow) also were reduced in Slc26a9$^{-/-}$ stomachs (Fig. 2*A Center* vs. *Left*). The cell area and nuclear area of parietal cells from Slc26a9$^{+/+}$, Slc26a9$^{+/-}$, and Slc26a9$^{-/-}$ mice were not significantly different. The thickness of the epithelium was increased significantly in Slc26a9$^{-/-}$ stomachs, and mucus cells contained numerous hyaline granules (Fig. 2*A*, dark blue arrow).

The ultrastructure of parietal cells, which were identified by virtue of their long and flexible apical microvilli and canalicular nidi, was analyzed by electron microscopy (Fig. 2*B*). There was a distinct absence of tubulovesicles in Slc26a9$^{-/-}$ parietal cells relative to those of Slc26a9$^{+/+}$ mice (Fig. 2*B*). Total secretory mem-

Author contributions: J.E., U.S., and M.S. designed research; J.X., P.S., M.L.M., F.B., S.B., B.R., and Z.W. performed research; S.L.A. and J.G.F. contributed new reagents/analytic tools; J.X., M.L.M., G.E.S., J.E., U.S., and M.S. analyzed data; and M.S. wrote the paper.

The authors declare no conflict of interest.

This article is a PNAS Direct Submission.

Freely available online through the PNAS open access option.

[1]J.X. and P.S. contributed equally to this work.

[2]Present address: Key Lab of Combined MultiOrgan Transplantation, Ministry of Public Health, The First Affiliated Hospital, School of Medicine, Zhejiang University, Hangzhou 310003, People's Republic of China.

[3]To whom correspondence should be addressed. E-mail: manoocher.soleimani@uc.edu.

This article contains supporting information online at www.pnas.org/cgi/content/full/0800616105/DCSupplemental.

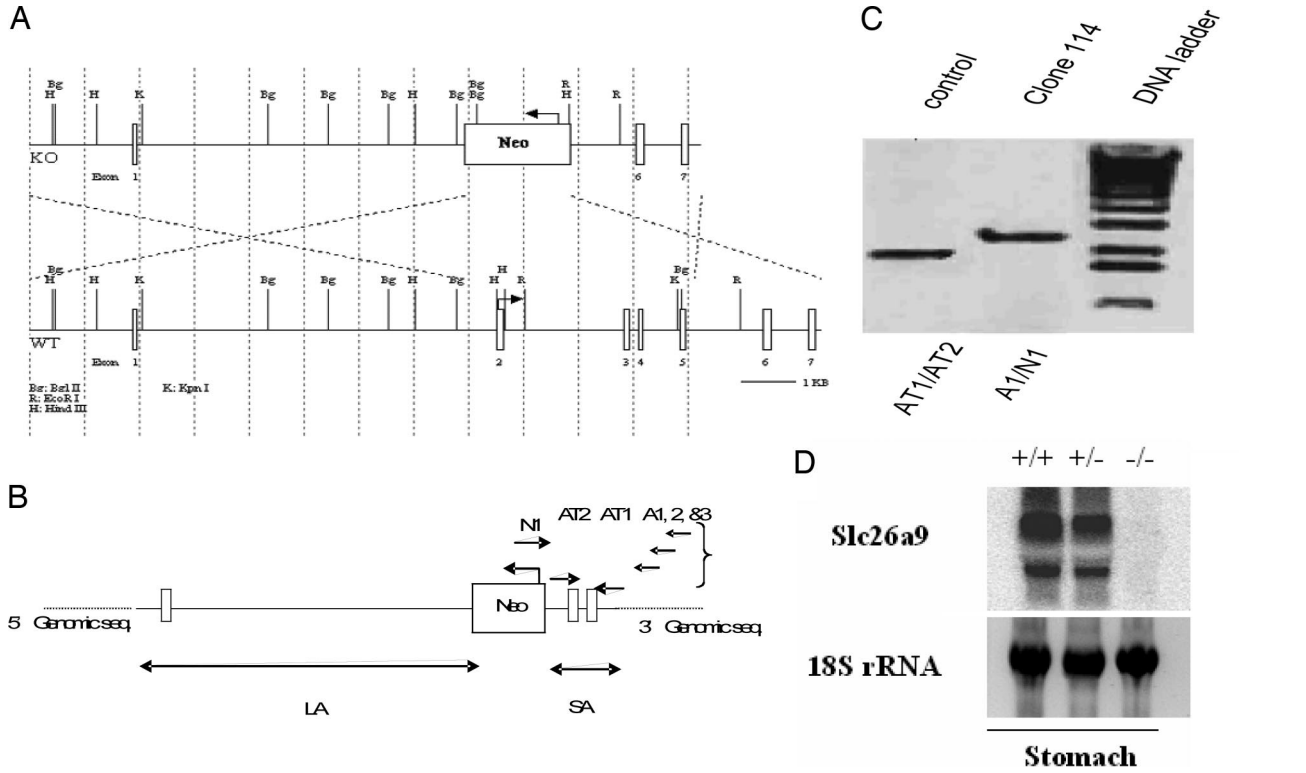

Fig. 1. Generation of Slc26a9$^{-/-}$ mutant mice. (*A*) A schematic of the Slc26a9 targeting construct. The Neo cassette replaces 4.0 kb of the gene, including exons 2–5 (and including the ATG start codon). (*B*) Slc26a9 targeting allele and delineation of locations of primers. Using primers designated A1, A2, and A3, which are downstream (3′) of the short homology arm (SA), PCRs were performed in conjunction with a primer at the 5′ end of the Neo cassette (referred to as N1). These reactions were expected to amplify 2.1-, 2.2-, and 2.3-kb fragments, respectively. The control PCR was done using AT1 and AT2, which are at the 5′ end of the SA inside the region used to create the targeting construct. This amplifies a band of 2.0 kb. The sequence for each primer is as follows: A1, 5′-tcacatgtgacttctggtcccattgg-3′; A2, 5′-tcacatagtggccatagaacac-3′; A3, 5′-tttcccagatcccactgtcttgc-3′; AT1, 5′-caccacaatcatctctgtagg-3′; AT2, 5′-tctgatggagctatcttgacc-3′ and N1, 5′-tgcgaggccagaggccacttgtgtagc-3′. (*C*) Identification of homologous recombinant clones. PCR analysis of DNA isolated from 200 surviving colonies identified an individual clone (clone 114) that showed homologous recombination. Southern blotting confirmed the results. The positive control was performed using primers AT1/N1, which gave the expected fragment size of 1.8 kb. (*D*) Generation of Slc26a9-null mice. Crossing of male chimera with female wild-type mice resulted in the generation of several heterozygote animals. Crossing of male and female Slc26a9 heterozygote mice (+/−) resulted in the generation of Slc26a9 KO mice. Northern hybridization on RNA isolated from the stomachs and lungs of Slc26a9 +/+, +/−, and −/− mice is shown. The expression of Slc26a9 is completely absent in the Slc26a9-null mouse. Slc26a9$^{-/-}$ mice exhibited normal growth, fertility, and survival compared with the wild-type littermates.

branes (apical microvilli, canalicular microvilli, and tubulovesicles together) were significantly reduced in Slc26a9$^{-/-}$ stomachs compared with those of control animals (WT, 87.5 ± 0.68 vs. KO, 64.5 ± 0.74). Mitochondria were plentiful and appeared to be normal in Slc26a9$^{-/-}$ stomachs. Similarly, the basal lamina, basement membrane, and intercellular interdigitations seemed normal in Slc26a9$^{-/-}$ stomachs.

Impaired Gastric Acid Secretion in Slc26a9-Null Mutant Mice. Given the remarkable histological alterations in mutant mice, we next examined acid secretion by measuring the pH and amount of acid or base in gastric secretions from Slc26a9$^{+/+}$ and Slc26a9$^{-/-}$ mice at ≈5–6 weeks of age after stimulation of acid secretion with histamine. The pH of gastric secretions was significantly more alkaline in Slc26a9$^{-/-}$ mice, with values of 6.4 ± 0.2 in Slc26a9$^{-/-}$ mice vs. 3.1 ± 0.2 in Slc26a9$^{+/+}$ ($P < 0.001$; Fig. 3*A*). Quantitation of gastric acid revealed no acid secretion in Slc26a9$^{-/-}$ mice (75 ± 6 meq/g of wet weight in Slc26a9$^{+/+}$ and 2 ± 0.7 meq/g in Slc26a9$^{-/-}$ mice; $P < 0.0001$; Fig. 3*B*). Western blot analyses were performed on membrane proteins isolated from the corpus of the stomach and showed that the abundance of gastric H-K-ATPase decreased by ≈55% in 5- to 6-week-old Slc26a9$^{-/-}$ mice ($n = 4$, $P < 0.05$; Fig. 3*C*).

Examination of gastric acid secretion in 17- to 19-day-old mice indicated that the pH of gastric contents was 2.9 ± 0.3 in Slc26a9$^{+/+}$ mice vs. 4.4 ± 0.3 in Slc26a9$^{-/-}$ mice ($n = 4$; $P < 0.01$). Gastric acid secretion was quantitated at 63 ± 7 meq/g of wet weight in Slc26a9$^{+/+}$ and 32 ± 6 meq/g of wet weight in Slc26a9$^{-/-}$ mice ($n = 7$, $P < 0.03$; Fig. 3*D*). Western blot analyses demonstrated that the abundance of gastric H-K-ATPase in 17- to 19-day-old Slc26a9$^{-/-}$ mice was similar to that of 5- to 6-week-old Slc26a9$^{+/+}$ mice (data not shown).

Expression of Parietal Cell Markers. To examine the basis of achlorhydria in Slc26a9-null mice, expression of AE2 and Slc26a7, which transport bicarbonate across the basolateral membrane (6–8, 26), and gastric H-K-ATPase was examined by Northern hybridization. Expressions of H-K-ATPase α subunit, AE2, and Slc26a7 mRNAs decreased by 45%, 42%, and 35%, respectively, in Slc26a9$^{-/-}$ stomachs [supporting information (SI) Fig. S1 *A–C*]. Expression of gastrin increased by 65% in Slc26a9$^{-/-}$ mice (Fig. S1*D*). Expression of ClC-2 mRNA decreased by 48% and its protein abundance decreased by ≈57% in adult mutant mice (Fig. S1 *E* and *F*).

Double-Immunofluorescence Labeling of Gastric H-K-ATPase and AE2. To probe the basis of the acid secretion defect further, double-immunofluorescence labeling was performed using AE2 and gastric H-K-ATPase β-subunit monoclonal antibodies. Fig. 4*A* *Upper* shows the expression of AE2 (*Left*) and gastric H-K-ATPase (*Right*) and the merged image (*Center*) in Slc26a9$^{+/+}$ mouse stomach. Fig.

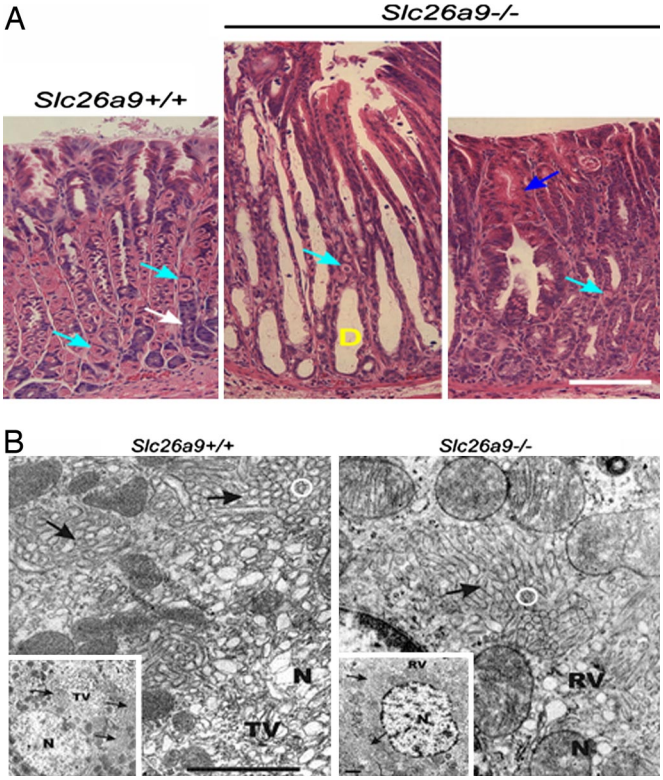

Fig. 2. Histopathologic and ultrastructural changes in Slc26a9-null gastric mucosa. (*A*) H&E staining shows gastric glands in the Slc26a9$^{-/-}$ mouse as dilated (D indicates dilated gastric gland) and containing lucent contents, which did not appear eosinophilic or basophilic, and small amounts of cellular debris (*Center* and *Right*) vs. Slc26a9$^{+/+}$ mice (*Left*). Parietal cell numbers were decreased in Slc26a9$^{-/-}$ mice (blue arrows). Zymogen cells were significantly reduced in Slc26a9$^{-/-}$ stomach (*Right*, white arrow). Mucous cells in Slc26a9$^{-/-}$ stomach contained a significant amount of hyaline granules (*Right*, dark blue). (*B*) Electron microscopy shows parietal cell ultrastructure. There was a distinct and striking absence of tubulovesicles (TV) in parietal cells in Slc26a9$^{-/-}$ (*Right*) vs. Slc26a9$^{+/+}$ stomach (*Left*). In place of tubulovesicles, parietal cells in Slc26a9$^{-/-}$ mice had abundant amounts of round vesicles (RV), which could be a premature or undeveloped form of tubulovesicle. *Insets* show a low-magnification image of part of a parietal cell, including nucleus (N), mitochondria, and areas of secretory membranes [canaliculi (black arrows) and tubulovesicles in the WT, and canaliculi (black arrows) and round vesicles in the KO]. The higher-magnification images of secretory membranes of the WT and KO are labeled similarly. The flattened tubulovesicles typical of the WT parietal cell were replaced by round vesicles in the KO. The white circle in each of the main figures surrounds a cross-section of a microvillus. In the WT the actin filaments in the microvillus are largely found peripherally and in close proximity to the plasma membrane, but in the KO the actin filaments are centrally located in a core. (Scale bars: *A*, 100 μm for light micrographs; *B*, 1 μm for electron micrograph.)

4*A Lower* shows the expression of these transporters in Slc26a9$^{-/-}$ stomachs. A larger magnification of the merged AE2/H-K-ATPase image is shown in Fig. 4*B*. Gastric H-K-ATPase staining in wild-type stomach displays a normal intracellular localization (Fig. 4*B Left*). An intriguing finding is the exclusive localization of H-K-ATPase on the apical pole of gastric parietal cells in Slc26a9$^{-/-}$ stomach (Fig. 4*B Right*), suggesting that there is little expansion of the secretory canaliculus within null mutant cells. The number of parietal cells is decreased by ≈43% in Slc26a9$^{-/-}$ mice ($n = 4$, $P < 0.01$), which would not account for the complete absence of acid secretion.

Immunoblot Analysis of Slc26a9 in Tubulovesicle Membranes of Gastric Parietal Cells. The expression of Slc26a9 in tubulovesicle membranes from gastric parietal cells was examined next. As shown in

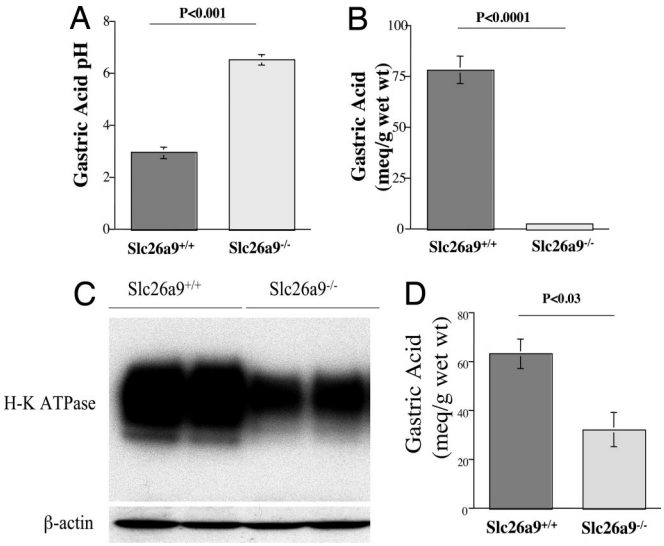

Fig. 3. Gastric acid secretion in Slc26a9$^{+/+}$ and Slc26a9$^{-/-}$ mice. Animals were fasted overnight, and gastric acid secretion was measured after s.c. injection of histamine according to *Experimental Procedures*. (*A*) Gastric acid pH in Slc26a9$^{+/+}$ and Slc26a9$^{-/-}$ mice (5–6 weeks old). The pH of the gastric secretions was significantly more alkaline in 5- to 6-week-old Slc26a9$^{-/-}$ mice. (*B*) Gastric acid secretion in Slc26a9$^{+/+}$ and Slc26a9$^{-/-}$ mice (5–6 weeks old). Acid secretion was decreased by ≈98% in Slc26a9$^{-/-}$ vs. Slc26a9$^{+/+}$ mice. (*C*) Western blotting of H-K-ATPase in the stomachs of 5- to 6-week-old Slc26a9$^{+/+}$ and Slc26a9$^{-/-}$ mice. (*D*) Gastric acid secretion in Slc26a9$^{+/+}$ and Slc26a9$^{-/-}$ mice (17–19 days old). The quantitation of gastric acid secretion in 17- to 19-day-old mice demonstrated ≈49% reduction in Slc26a9$^{-/-}$ mice.

Fig. 4*C*, lane 1, a ≈92-kDa band was detected in a fraction blotted against the Slc26a9 antibody. Preadsorption of the antibody with the synthetic peptide prevented the labeling of the ≈92-kDa band (Fig. 4*C*, lane 2).

Next, we examined the functional properties of mouse Slc26a9 in oocytes and mammalian cultured cells. Our results demonstrate that in oocytes Slc26a9 functions as an anion-conductive pathway with a high affinity for chloride (Fig. S2*A*). In COS7 cells transiently transfected with Slc26a9, pH_i recordings demonstrated enhanced Cl^-/HCO_3^- exchange activity vs. sham-transfected cells (Fig. S2*B*).

The pH-Stat Titration of Acid Secretion in Isolated Gastric Mucosa from 7- to 9-Day-Old or 40- to 45-Day-Old Mice. To quantify the actual rates of HCl secretion, isolated gastric mucosae from Slc26a9$^{-/-}$, Slc26a9$^{+/-}$ and Slc26a9$^{+/+}$ mice were studied in modified Ussing chamber systems. In 40- to 45-day-old mice, the gastric mucosae from Slc26a9$^{-/-}$ mice did not exhibit spontaneous or forskolin-stimulated acid secretory rates (Fig. 5*C*). Interestingly, Slc26a9 heterozygous mice had significantly lower acid secretory peak rates relative to wild-type mice (Fig. 5*A*).

We found spontaneous acid secretion in 7- to 9-day-old mice (i.e., more acid than HCO_3^- flux into the lumen), which could be stimulated by the addition of 10^{-5} M forskolin to the serosal perfusate (Fig. 5*B*). In 7- to 9-day-old mice there was no statistically significant difference between basal and forskolin-stimulated acid secretory rates in Slc26a9-null, heterozygous, or wild-type gastric mucosae (Fig. 5*B*).

The above experiments in adult mice were repeated, with 70 mM NaCl in the perfusate being replaced with KCl. The objective was to determine whether a high concentration of K^+ in the perfusate could rescue the acid secretion defect in Slc26a9$^{-/-}$ mice. This concentration of KCl was chosen based on our finding that it provides optimal secretory rates when compared with 30 or 154 mM luminal KCl (Fig. S3).

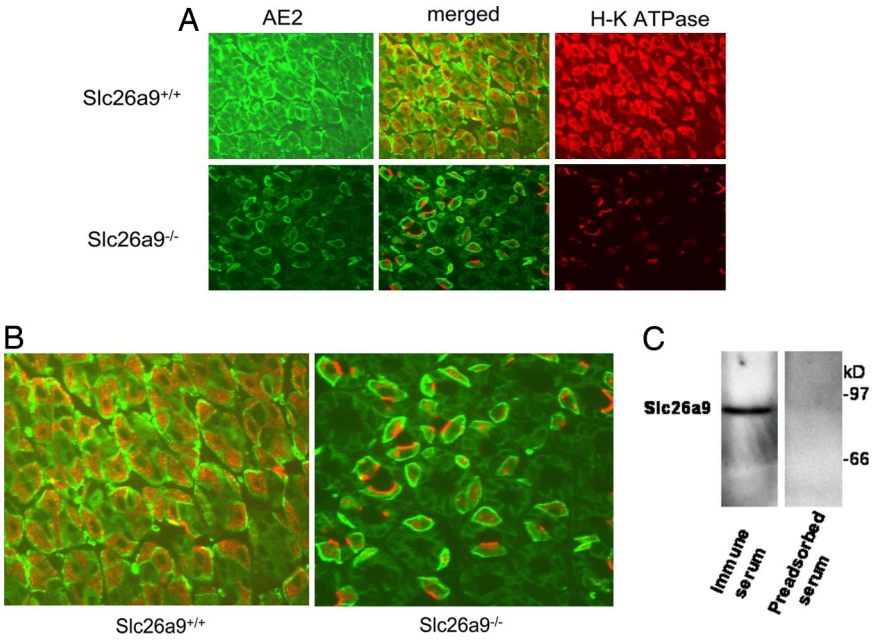

Fig. 4. Expression of AE2 and H-K-ATPase and localization of Slc26a9 in parietal cells. (*A*) Expression of AE2 and gastric H-K-ATPase (low magnification). (*Upper*) Expression of AE2 (*Left*) and gastric H-K-ATPase (*Right*) in wild-type mouse stomach. *Center* shows a merged image. (Lower) Expression of AE2 (*Left*) and gastric H-K-ATPase (*Right*), along with the merged image (*Center*), in an Slc26a9-null mouse. (*B*) Expression of AE2 and gastric H-K-ATPase (high magnification). AE2/H-K-ATPase merged images in the stomachs of Slc26a9$^{+/+}$ (*Left*) and Slc26a9$^{-/-}$ (*Right*) mice are shown. Contrary to wild-type animals, H-K-ATPase labeling in Slc26a9-null mice was detected almost exclusively on the apical pole of gastric parietal cells, with little intracellular localization (*Right*). (Original magnifications; A, 100×; B, 400×.) (*C*) Western blotting of Slc26a9 in tubulovesicles isolated from gastric parietal cells. Western blotting detected a specific band in tubulovesicles isolated from gastric parietal cells. Left lane, immune serum; right, preadsorbed serum.

There was an initial increase in basal acid secretion in the presence of increased perfusate KCl, which was further increased in response to forskolin in Slc26a9$^{+/+}$ mice (Fig. 5*C*). Slc26a9$^{-/-}$ mice, however, had a complete absence of gastric acid secretion in the basal state in the presence of increased perfusate KCl and in response to forskolin (Fig. 5*C*). There was

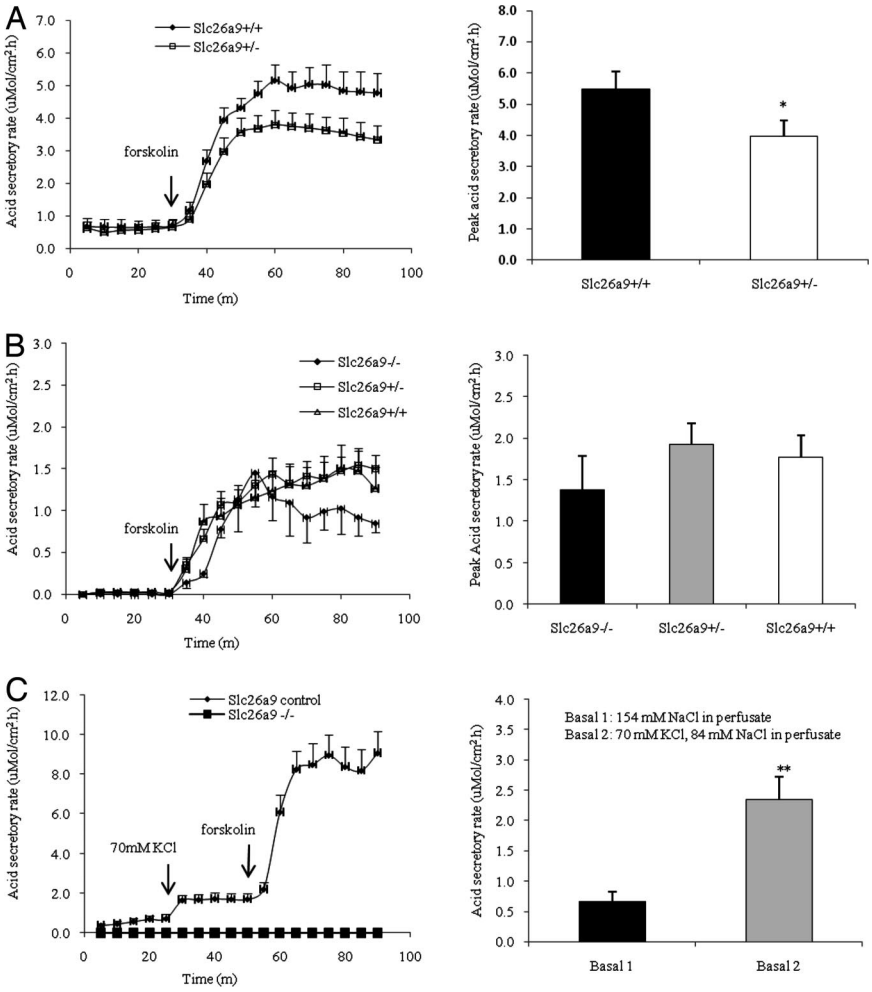

Fig. 5. Time course (*Left*) and peak acid secretory rates (*Right*) in isolated gastric mucosa. (*A* and *B*) The 40- to 45-day-old (*A*) and 7- to 9-day-old (*B*) Slc26a9$^{-/-}$, Slc26a9$^{+/+}$, and Slc26a9$^{+/-}$ mice. (*C*) Effect of high-potassium perfusate on acid secretion in Slc26a9$^{+/+}$ and Slc26a9$^{-/-}$ mice. Acid secretion was measured at basal state and after the stimulation with forskolin (10^{-5} M) in the gastric mucosa of the mice. Acid secretion was completely absent in adult Slc26a9$^{-/-}$ mice (*C*), and peak secretion was significantly lower in Slc26a9$^{+/-}$ relative to Slc26a9$^{+/+}$ mucosa (n = 9 for +/+, 13 for +/−, and 4 for −/− mice) (*A*). No significant difference was observed between stomachs of 7- to 9-day-old Slc26a9$^{-/-}$, +/+, and +/− mice (n = 5 for −/−, 11 for +/+, and 17 for +/−. Acid secretion at basal state and in response to forskolin was examined in the presence of perfusate NaCl or KCl in Slc26a9$^{+/+}$ and Slc26a9$^{-/-}$ mice (*C*).

no acid secretion in Slc26a9$^{+/+}$ mice in the absence of chloride in the perfusate (Fig. S4).

Discussion

There are 2 components of the luminal chloride secreted by parietal cells: the acidic component of Cl^- secretion, which is essential for gastric HCl secretion, and the nonacidic component, which is observed as a transmucosal movement of Cl^- in excess of H^+ (8, 9, 32). Cl^- secretion is required for H^+ secretion because it is needed to balance the current generated by secretion of K^+, which serves as a substrate of the H-K-ATPase. K^+ secretion, which probably occurs via Kir4.1, Kir2.1, and/or KCNQ1, provides the luminal K^+ that is required as a counterion for H^+/K^+ exchange by the gastric H-K-ATPase.

Slc26a9-null mice displayed achlorhydria along with the absence of tubulovesicles in gastric parietal cells. The impairment of gastric acid secretion was evident as early as 17 days after birth and before any significant reduction in the number of parietal cells was apparent (*Results*). The expression of Slc26a9 in tubulovesicles establishes a causal link between Slc26a9 deletion and the impairment of gastric acid secretion. Slc26a9 can function as anion conductive pathway as well as Cl^-/HCO_3^- exchanger (Fig. S2) (27, 29, 30). In either mode, Slc26a9 has the potential to regulate gastric acid secretion.

Although the functional presence of Cl^-/HCO_3^- exchange in tubulovesicle membranes has been documented (33), conceiving of a physiological function for such an activity in the secretory canaliculus during acid secretion is difficult. However, such an activity could play an important role in H-K-ATPase-containing membranes immediately after the transition from the stimulated to the resting state and also in resting tubulovesicles. Striking electron micrographs by Ito *et al.* (34) demonstrate that transition of the parietal cell to the resting state can result in closing of the apical opening to the lumen of the gland while extended canaliculi remain within the cell. No mechanism has been proposed by which the voluminous acid contents of these entirely intracellular canaliculi could be dissipated. If an anion exchanger were present in these structures, then its Cl^-/HCO_3^- exchange activity might provide a mechanism for removing HCl and, ultimately, dehydrating the canaliculus. Similarly, because the H-K-ATPase is retrieved from the canalicular membranes by endocytosis, the lumen of the tubulovesicles would remain acidic if there were no transport mechanism, such as Cl^-/HCO_3^- exchange, for removal of HCl. It is therefore plausible that Slc26a9 can maintain the viability of tubulovesicles by functioning as a Cl^-/HCO_3^- exchanger, therefore neutralizing the acidic pH and removing Cl^- from the canaliculus during transition to the resting state.

Alternatively, Slc26a9 could play a major role in gastric acid secretion by functioning as a Cl^- conductive pathway. Despite the essential role of the apical Cl^- channel in gastric acid secretion, its molecular identity remains unclear and controversial. Slc26a9 is a reasonable candidate as a parietal cell Cl^- conductive pathway for the following reasons: It is expressed in tubulovesicles and functions as a Cl^- channel in some expression systems, and its deletion has profound effects on tubulovesicle abundance and acid secretion in both very young and adult mice. It should be noted, however, that 7-day-old Slc26a9$^{-/-}$ mice had low but comparable gastric acid secretion relative to wild-type littermates. The ontogeny of gastric acid secretion in rodents showed that major developmental changes in the acid secretory response to secretagogues occur during this period (35, 36). Interestingly, measurements of acid secretion showed a sharp increase in the rate of acid secretion between birth and 5 days of age, followed by a decrease at 10–15 days but a further increase by day 18 (36). Although highly speculative at this point, an early developmental switch in the specific Cl^- conductive pathway expressed in secretory membranes is a possible reason for the normal acid secretion in 7-day-old mice and the loss of acid secretion in older animals.

Despite the evidence in favor of Slc26a9 functioning as the major gastric Cl^- channel in juvenile and adult mice, our data do not unambiguously support this conclusion. We expected that the addition of KCl to the luminal bath would stimulate H-K-ATPase activity; however, contrary to our hypothesis, luminal acidification was not observed in the stomachs of 5- to 6-week-old Slc26a9$^{-/-}$ mice. In addition to (or as an alternative to) a direct role in acid secretion, Slc26a9 deletion could have indirect effects on acid secretion by impairing the viability of parietal cells or the development of secretory membranes, as observed in Figs. 2 and 4 (*Results*).

Another interesting aspect of the study was the reduction in the acid secretory capacity of the adult heterozygotes. A similar situation has been found for intestinal Cl^- and fluid secretion in mice heterozygous for null mutations in the cystic fibrosis transmembrane conductance regulator (CFTR) (37), and was later confirmed in the nasal epithelium of humans who are heterozygous for cystic fibrosis mutations (38). These observations suggest that Slc26A9 is rate-limiting for acid secretion, at least in adult mice, and further indicate that it plays a major role in HCl secretion.

In conclusion, Slc26a9 deletion results in decreased gastric acid secretion and the loss of tubulovesicles at a young age and reduction in parietal cells in adult mice. We propose that Slc26a9 plays an essential role in gastric acid secretion by regulating chloride secretion and/or by affecting the viability or maturation or tubulovesicles/secretory canaliculi in parietal cells.

Experimental Procedures

Preparation of Targeting Construct, Embryonic Stem (ES) Electroporation, and Generation of Mutant Mice. A ≈14.3-kb region used to construct the targeting vector was first subcloned from a BAC clone. The region was designed such that the short homology arm (SA) extends ≈2.4 kb 3′ to Neo cassette. The long homology arm (LA) starts at the 5′ side of the Neo cassette and is ≈7.7 kb long. The Neo cassette replaces 4.0 kb of the gene, including exons 2–5.

Ten micrograms of the targeting vector was linearized with NotI and then transfected by electroporation of 129 Sv/Ev ES cells. After selection in G418, surviving clones were expanded for PCR analysis to identify recombinant ES clones. One recombinant clone (clone 114) was identified.

Animals. Mice were cared for in accordance with the Institutional Animal Care and Use Committee (IACUC) at the University of Cincinnati and Hannover Medical School. All animal handlers were IACUC-trained. Animals were euthanized with the use of either anesthetics (pentobarbital sodium) or cervical dislocation after carbon dioxide narcosis according to institutional guidelines and approved protocols.

Histology and Electron Microscopy. For electron microscopy, stomachs were processed as described in ref. 31. Sections were either stained with toluidine blue or fixed in formalin, dehydrated, and embedded in paraffin. Sections 5 μm thick were stained with H&E, or with periodic acid–Schiff (PAS) and Alcian blue for light microscopy. Morphometric analysis of the glandular and forestomach epithelium was performed as described in ref. 31.

Parietal cells were required to contain a nuclear profile, predominant large and well-organized mitochondrial distribution, and visible lucent areas of smooth membranes (canaliculi and tubulovesicles). Zymogenic cells were identified as having a profile of nucleus, basophilic cytoplasm (RER), and a minimum of 3 birefringent granules. Mucus neck cells were dark and small, and mucus pit cells were determined by their mucus granules. The area of parietal cells and of parietal cell nuclei was also digitized (μm^2).

Measurement of Gastric pH and Acid/Base Equivalents. Mice were fasted overnight and euthanized 15 min after s.c. injection of histamine (2 μg/g of body weight), and the intact stomachs were removed. The gastric contents were rinsed into 5 mL of oxygen-saturated normal saline solution at room temperature, degassed, and pelleted by centrifugation, and the pH and acid/base equivalents were determined by titration with NaOH as described in ref. 31.

pH-Stat Titration of Acid Secretory Rates in Isolated Gastric Mucosa. For adult stomachs (45-day-old mice), the experimental maneuvers were similar to those published, with modifications as described in ref. 32. Briefly, the mucosal layer was dissected from mouse gastric corpus under a stereomicroscope and mounted between 2 Lucite half-chambers of a water-jacketed Ussing system equipped with

a gas-lift system. The exposed surface area was 0.283 cm^2. For the 7- to 9-day-old mice, the tiny stomachs were not stripped. The serosal solution contained (in mM) 108 NaCl, 22 $NaHCO_3$, 3 KCl, 1.3 $MgSO_4$, 2 $CaCl_2$, 2.25 KH_2PO_4, 8.9 glucose, and 10 sodium pyruvate, and was gassed with 95% O_2/5% CO_2 (pH 7.4). The chamber was allowed to equilibrate for at least 30 min in the presence of indomethacin (3 μM), and tetrodotoxin (1 μM) was added to the serosal solution to minimize the impact of intrinsic prostanoid and neural tone.

The mucosal solution (154 mM NaCl or 70 mM NaCl and 70 mM KCl) was gassed with 100% O_2 and maintained at pH 7.4 by the addition of dilute (2 mM) NaOH (in a 0.1-μL volume) using a pH-Stat titration system (Radiometer). Basal parameters were measured for 30 min and after addition of 10 μM forskolin to serosal solution. Acid secretory rates were recorded for 60 min at 5-min intervals.

RNA Isolation and Northern Blot Hybridization. Total cellular RNA was extracted from stomach, and hybridization was performed according to established protocols.

Immunofluorescent Labeling of AE2 and Gastric H-K-ATPase in Mouse Stomach. Single- and double-immunofluorescent labeling on frozen sections from stomachs was performed as described by using AE2 polyclonal and gastric H-K-ATPase (beta subunit) monoclonal antibodies as described (33).

Immunoblot Analysis of Slc26a9 in Tubulovesicles Isolated from Gastric Parietal Cells. Tubulovesicle membrane proteins, isolated from rabbit gastric parietal cells (33), were loaded (15 μg per lane), resolved by SDS/PAGE, and incubated with antibodies against Slc26a9 (27). The results were visualized by using chemiluminescence.

Western Blotting of Gastric H-K-ATPase and ClC-2 in the Stomach of Slc26a9$^{+/+}$ and Slc26a9$^{-/-}$ Mice. The corpus mucosa was dissected with a razor blade, washed, and centrifuged. Protein extracts were prepared as described (25–28) in the presence of a mixture of protease inhibitors. Western blotting was performed as above by using H-K-ATPase or ClC-2 polyclonal antibodies.

Slc26a9 Expression in Oocytes and Cultured Cells. Slc26a9 was subcloned into the plasmid pSP64poly(A) (Promega) downstream of the SP6 RNA promoter. The cRNA was produced by using the mMESSAGE mMACHINE SP6 (Ambion) and injected into collagenase-defolliculated oocytes from *Xenopus laevis* as described (39).

Two-electrode voltage-clamp measurements were performed at room temperature as described in ref. 39. Briefly, oocytes were voltage-clamped at a holding potential of −30 mV, and 800-ms voltage steps from −100 mV to +80 mV in 20-mV increments were applied by using a TEV 200 amplifier (Dagan) and were monitored by computer through Digidata 1200A/D converter and pCLAMP 6.0 software (Axon Instruments).

COS7 cells were transiently transfected with either mouse Slc26a9 cDNA or vector alone (sham transfection). Intracellular pH and the Cl^-/HCO_3^- exchange activity were recorded with the use of pH fluorescent probe BCECF (24).

PCR Screening of Slc26a9-Null and Wild-Type Mice. Tail DNA genotyping was performed using A1/N1 primer pair (see above in *Experimental Procedures*) to identify Slc26a9-null mice (sequences: A1, 5′-tcacatgtgacttctggtcccattgg-3′; and N1, 5′-tgcgaggccagaggccacttgtgtagc-3′). For wild type, AT1/AT2 primer pair (AT1, 5′-caccacaatcatctctgtagg-3′; and AT2, 5′-tctgatggagctatcttgacc-3′) was used.

Materials. Nitrocellulose filters and other chemicals were purchased from Sigma.

Statistical Analyses. Data for microcopy and morphometry were analyzed by using SigmaPlot (SigmaPlot) and means and standard errors, and unpaired *t* tests were determined by genotype and sex. Results were considered significant when $P \leq 0.05$.

ACKNOWLEDGMENTS. These studies were supported by a Merit review grant from the Department of Veterans Affairs, National Institutes of Health Grants DK62809 (to M.S.) and DK50594 (to G.E.S.), and the Deutsche Forschungsgemeinschaft Sachbeihilfe Se 460/9-5 and 9-6, the Ministry of Science in Lower Saxony, and the Volkswagen Stiftung (to U.S.).

1. Forte JG, Machen TE (1975) Transport and electrical phenomena in resting and secreting piglet gastric mucosa. *J Physiol* 244:33–51.
2. Berglindh T (1977) Absolute dependence on chloride for acid secretion in isolated gastric glands. *Gastroenterology* 73:874–880.
3. Machen TE, McLennan WL (1980) Na^+-dependent H^+ and Cl^- transport in in vitro frog gastric mucosa. *Am J Physiol* 238:G403–G413.
4. Muallem S, Burnham C, Blissard D, Berglindh T, Sachs G (1985) Electrolyte transport across the basolateral membrane of the parietal cells. *J Biol Chem* 260:6641–6653.
5. Paradiso AM, Tsien RY, Demarest JR, Machen TE (1987) Na-H and Cl-HCO_3 exchange in rabbit oxyntic cells using fluorescence microscopy. *Am J Physiol* 253:C30–C36.
6. Seidler U, Hübner M, Roithmaier S, Classen M (1994) pH_i and HCO_3^- dependence of proton extrusion and Cl^--base exchange rates in isolated rabbit parietal cells. *Am J Physiol* 266:G759–G766.
7. Hersey SJ, Sachs G (1995) Gastric acid secretion. *Physiol Rev* 75:155–189.
8. Gawenis LR, *et al.* (2004) Mice with a targeted disruption of the AE2 Cl^-/HCO_3^- exchanger are achlorhydric. *J Biol Chem* 279:30531–30539.
9. Coskun T, Baumgartner HK, Chu S, Montrose MH (2002) Coordinated regulation of gastric chloride secretion with both acid and alkali secretion. *Am J Physiol* 283:G1147–G1155.
10. Sherry AM, Malinowska DH, Morris RE, Ciraolo GM, Cuppoletti J (2001) Localization of ClC-2 Cl^- channels in rabbit gastric mucosa. *Am J Physiol* 280:C1599–C1606.
11. Malinowska DH, Sherry AM, Tewari KP, Cuppoletti J (2004) Gastric parietal cell secretory membrane contains PKA- and acid-activated Kir2.1 K^+ channels. *Am J Physiol* 286:C495–C506.
12. Hori K, *et al.* (2004) Is the ClC-2 chloride channel involved in the Cl^- secretory mechanism of gastric parietal cells? *FEBS Lett* 575:105–108.
13. Bosl MR, *et al.* (2001) Male germ cells and photoreceptors, both dependent on close cell-cell interactions, degenerate upon ClC-2 Cl^- channel disruption. *EMBO J* 20:1289–1299.
14. Bissig M, Hagenbuch B, Stieger B, Koller T, Meier PJ (1994) Functional expression cloning of the canalicular sulfate transport system of rat hepatocytes. *J Biol Chem* 269:3017–3021.
15. Hastbacka J, *et al.* (1994) The diastrophic dysplasia gene encodes a novel sulfate transporter: Positional cloning by fine-structure linkage disequilibrium mapping. *Cell* 78:1073–1087.
16. Schweinfest CW, Henderson KW, Suster S, Kondoh N, Papas TS (1993) Identification of a colon mucosa gene that is down-regulated in colon adenomas and adenocarcinomas. *Proc Natl Acad Sci USA* 90:4166–4170.
17. Everett LA, *et al.* (1997) Pendred syndrome is caused by mutations in a putative sulphate transporter gene (PDS). *Nat Genet* 17:411–422.
18. Zheng J, *et al.* (2000) Prestin is the motor protein of cochlear outer hair cells. *Nature* 405:149–155.
19. Lohi H, *et al.* (2000) Mapping of five new putative anion transporter genes in human and characterization of SLC26A6, a candidate gene for pancreatic anion exchanger. *Genomics* 70:102–112.
20. Lohi H, *et al.* (2002) Functional characterization of three novel tissue-specific anion exchangers SLC26A7, -A8, and -A9. *J Biol Chem* 277:14246–14254.
21. Vincourt JB, Jullien D, Amalric F, Girard JP (2003) Molecular and functional characterization of SLC26A11, a sodium-independent sulfate transporter from high endothelial venules. *FASEB J* 17:890–892.
22. Soleimani M (2006) Expression, regulation and the role of SLC26 Cl^-/HCO_3^- exchangers in kidney and gastrointestinal tract. *Novartis Found Symp* 273:91–102.
23. Melvin JE, Park K, Richardson L, Schultheis PJ, Shull GE (1999) Mouse down-regulated in adenoma (DRA) is an intestinal Cl^-/HCO_3^- exchanger and is up-regulated in colon of mice lacking the NHE3 Na^+/H^+ exchanger. *J Biol Chem* 274:22855–22861.
24. Soleimani M, *et al.* (2001) Pendrin: An apical $Cl^-/OH^-/HCO_3^-$ exchanger in the kidney cortex. *Am J Physiol* 280:F356–F364.
25. Wang Z, Petrovic S, Mann E, Soleimani M (2002) Identification of an apical Cl^-/HCO_3^- exchanger in the small intestine. *Am J Physiol* 282:G573–G579.
26. Petrovic S, *et al.* (2003) Identification of a basolateral Cl^-/HCO_3^- exchanger specific to gastric parietal cells. *Am J Physiol* 284:G1093–G1103.
27. Xu J, *et al.* (2005) SLC26A9 is expressed in gastric surface epithelial cells, mediates Cl^-/HCO_3^- exchange, and is inhibited by NH_4^+. *Am J Physiol* 289:C493–C505.
28. Kim KH, Shcheynikov N, Wang Y, Muallem S (2005) SLC26A7 is a Cl^- channel regulated by intracellular pH. *J Biol Chem* 280:6463–6470.
29. Dorwart MR, Shcheynikov N, Wang Y, Stippec S, Muallem S (2007) SLC26A9 is a Cl^- channel regulated by the WNK kinases. *J Physiol* 584:333–345.
30. Romero MF, *et al.* (2006) Physiology of electrogenic SLC26 paralogues. *Novartis Found Symp* 273:126–138.
31. Schultheis PJ, *et al.* (1998) Targeted disruption of the murine Na^+/H^+ exchanger isoform 2 gene causes reduced viability of gastric parietal cells and loss of net acid secretion. *J Clin Invest* 101:1243–1253.
32. McDaniel N, *et al.* (2005) Role of Na-K-2Cl cotransporter-1 in gastric secretion of nonacidic fluid and pepsinogen. *Am J Physiol* 289:G550–G560.
33. Petrovic S, *et al.* (2002) Colocalization of the apical Cl^-/HCO_3^- exchanger PAT1 and gastric H-K-ATPase in stomach parietal cells. *Am J Physiol* 283:G1207–G1216.
34. Ito S, Munro DR, Schofield GC (1977) Morphology of the isolated mouse oxyntic cell and some physiological parameters. *Gastroenterology* 73:887–898.
35. Ackerman SH (1982) Ontogeny of gastric acid secretion in the rat: Evidence for multiple response systems. *Science* 217:75–77.
36. Seidel ER, Johnson LR (1984) Ontogeny of gastric mucosal muscarinic receptor and sensitivity to carbachol. *Am J Physiol* 9:G550–G555.
37. Gabriel SE, Brigman KN, Koller BH, Boucher RC, Stutts MJ (1994) Cystic fibrosis heterozygote resistance to cholera toxin in the cystic fibrosis mouse model. *Science* 266:107–109.
38. Sermet-Gaudelus I, *et al.* (2005) Chloride transport in nasal ciliated cells of cystic fibrosis heterozygotes. *Am J Respir Crit Care Med* 171:1026–1031.
39. Schmieder S, Lindenthal S, Banderali U, Ehrenfeld J (1998) Characterization of the putative chloride channel xClC-5 expressed in Xenopus laevis oocytes and comparison with endogenous chloride currents. *J Physiol* 511:379–393.